A mixture of ferritin and magnetite nanoparticles mimics the magnetic properties of human brain tissue

Franziska Brem,[1] Louis Tiefenauer,[2] Alke Fink,[3] Jon Dobson,[4] and Ann M. Hirt[1,*]
[1]*Institute of Geophysics, ETH Zurich, 8093 Zurich, Switzerland*
[2]*Paul Scherrer Institut, 5232 Villigen PSI, Switzerland*
[3]*Laboratory of Powder Technology, EPFL Lausanne, Switzerland*
[4]*Institute for Science and Technology in Medicine, Keele University, Stoke-on-Trent ST4 7QB, United Kingdom*
(Received 6 February 2006; revised manuscript received 28 April 2006; published 20 June 2006)

Magnetic properties of a two-component system, consisting of horse spleen ferritin (HoSF) which contains a 5–8 nm sized antiferromagnetic ferrihydrite ($5Fe_2O_3 \cdot 9H_2O$) core and ferrimagnetic magnetite (Fe_3O_4) nanoparticles (MNP) with an average size of 10–20 nm, have been investigated by using four different methods: induced magnetization versus (1) temperature and (2) field; (3) AC susceptibility; and (4) first-order reversal curves (FORC). All measurements were done on a mixed system of HoSF and MNP, as well as separately on the individual components. The average blocking temperature (T_B) of the mixed system at 50 mT is 15.6 K, which is a shift towards higher temperatures compared to pure HoSF ($T_B = 12$ K). The contribution of the MNP component to magnetic ordering is evident only as a separation of the zero-field-cooled and field-cooled measurement curves. ac susceptibility is dominated by the ferrimagnetic MNP and shows strong frequency dependence. The peak ac susceptibilities can be described by the Vogel-Fulcher law, indicating the influence of interactions within the system. Hysteresis measurements at 5 K show a wasp-waisted shape due to the mixture of a high coercivity phase (HoSF) with a low coercivity phase (MNP). Initial magnetization curves above T_B can be fitted by a sum of Langevin functions, showing superparamagnetic behavior of both components. FORC diagrams are effective in illustrating the change from that of blocked MNP particles together with the superparamagnetic HoSF at 20 K to purely superparamagnetic behavior in both components above 50 K. We conclude that the mixed nanoparticle system is a good model for complex natural samples, such as human brain tissue.

DOI: 10.1103/PhysRevB.73.224427 PACS number(s): 75.50.Tt, 75.50.−y, 76.60.Es

I. INTRODUCTION

Characterization of magnetic properties can offer valuable information for investigations of the history and function of materials. Natural systems, such as soils, rocks, and diverse biological materials, usually contain more than one magnetic component. Furthermore, synthetic materials may also contain more than one magnetic component due to by-products of synthesis or chemical oxidation processes.[1,2] Such mixed systems are rarely described, because measurements of their physical properties are difficult to interpret and various methods of analysis are usually needed to separate and characterize each contributing component. Even more difficult to characterize are mixtures consisting of different nanosized magnetic particles. One unusual example of such a complex magnetic mixture is tissue from the human brain. The interest in iron metabolism and iron components found in the human brain has increased strongly in the past few years because of their association with neurological and neurodegenerative diseases.[3] Human brain tissues contain at least four different magnetic components. The dominant magnetic signal arises from the strongly diamagnetic fatty tissue (the matrix) in which the other components are embedded. The second dominant component is heme-iron from blood, which is near paramagnetic in its magnetic properties.[4] Ferritin, the third component, which is responsible for the intracellular storage of iron, is present throughout the brain. Ferritin consists of a core of antiferromagnetic ferrihydrite ($5Fe_2O_3 \cdot 9H_2O$), 5–8 nm in diameter, surrounded by a protein shell,[5] and is superparamagnetic at room temperature. In the past decade magnetite/maghemite (Fe_3O_4/γ-Fe_2O_3) has been discovered in human brain tissue.[6,7] The origin and the formation process of this strongly ferrimagnetic component are still unknown and the subject of intense research. Identification of the different magnetic components is difficult, and magnetic modeling is nearly impossible, since the concentrations of the individual phases and their iron contents are unknown.

To gain a better physical understanding of such multicomponent magnetic systems, we measured two known magnetic components separately and as a mixture. This system consists of commercially available horse spleen ferritin (HoSF), which is magnetically well characterized,[8–10] and albumin coated magnetite nanoparticles (MNP) with 10–20 nm diameter. Both components are superparamagnetic at room temperature. Therefore, measurements at low temperature are required for a full magnetic characterization of the mixed system HoSF-MNP. This model will facilitate the characterization of natural multicomponent systems of biological origin.

II. EXPERIMENTAL DETAILS

The MNP sample was made from 300 mg magnetite nanoparticles with a diameter of 10–20 nm suspended in 10 mM HCl. This material was originally developed as a contrast agent for magnetic resonance imaging.[11,12] The particles were then coated with 150 mg poly-(D-glutamic acid,

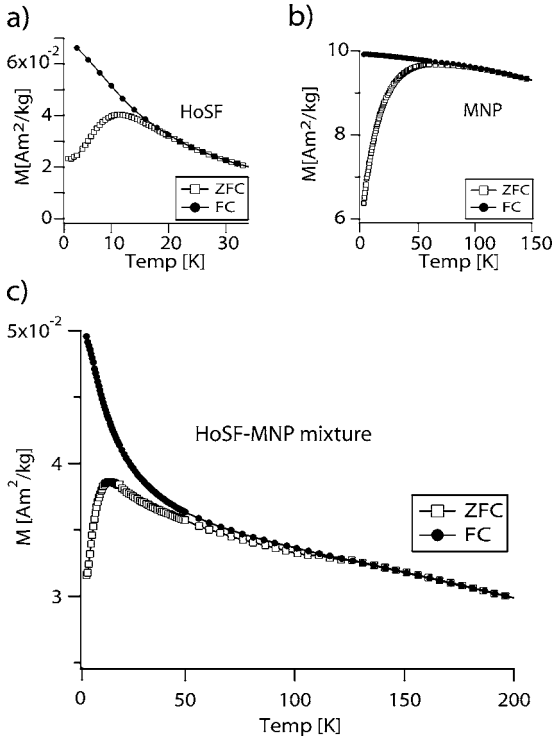

FIG. 1. Induced magnetization as a function of temperature measured after zero-field cooling (ZFC) and cooling in a 50 mT field (FC) of (a) pure HoSF, (b) pure MNP, and (c) HoSF-MNP mixed system.

D-lysine) hydrobromide (6:4) (wt. 20–50 kD, from Sigma) in 100 mM HEPES pH 6.8, washed with 100 mM HEPES pH 7.3 and ultrasonically dispersed. Finally, coated particles were incubated for 30 min in 1 ml 0.1% human serum albumin. After washing, the material was lyophilized and the resulting dry powder was mixed with commercial horse spleen ferritin (HoSF, Sigma). The ferritin-magnetite mixture was dried and packed into a gel cap for handling. The

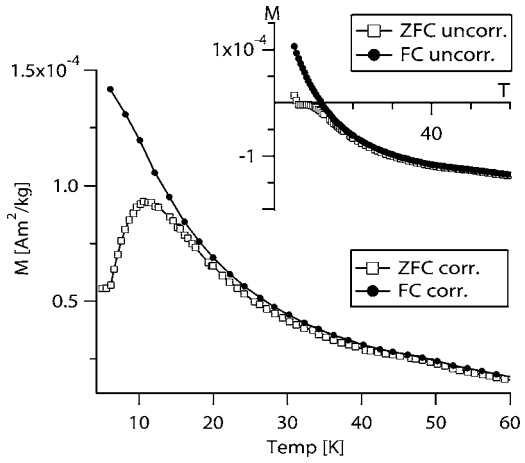

FIG. 2. Induced magnetization as a function of temperature after ZFC and FC at 50 mT of a human brain tissue sample, corrected for the diamagnetic matrix signal and the paramagnetic blood signal. The inset shows the uncorrected induced magnetization for the same sample.

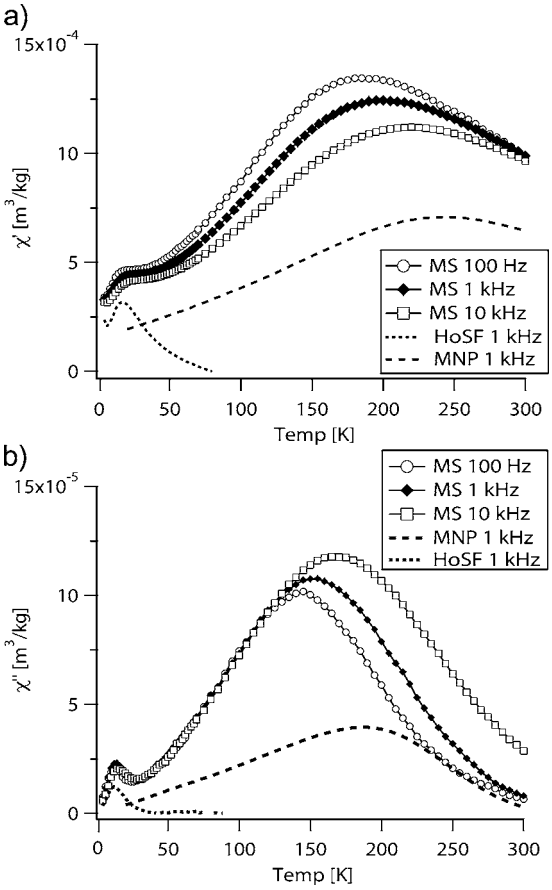

FIG. 3. In-phase susceptibility χ' (a) and out-of-phase susceptibility χ'' (b) as a function of temperature. The HoSF-MNP mixed system was measured at frequencies of 100 Hz, 1 kHz, and 10 kHz. The dotted lines indicate (a) χ' and (b) χ'' for the pure components HoSF and MNP, measured at 1 kHz.

samples contain 60–70 mg of HoSF and 0.4–0.5 mg of MNP. These low concentrations were chosen to mimic the assumed natural content in biological samples.

Induced magnetization was measured as a function of both temperature and field using a Quantum Design MPMS superconducting quantum interference device (SQUID) magnetometer at the University of Bremen and at the Chemistry Department at ETH Zurich. In the thermal experiments, samples were initially cooled to 5 K, either in the absence of a magnetic field (zero-field cooling, ZFC) or in the presence of a 50 mT field (field cooling, FC). At 5 K a magnetic field of 50 mT was applied and the induced magnetic moment of the sample was measured at intervals of 2 K during heating to 300 K. The sample magnetization was also measured as a function of field (hysteresis loops and initial magnetization curves) at a series of temperatures between 5 and 300 K, in fields of ±5 T after cooling the samples in zero field. ac susceptibility measurements were made at different frequencies between 100 Hz and 10 kHz in a weak applied field of 79.7 A m (1 Oe) on a Quantum Design Physical Property Measurement System (PPMS) at the Chemistry Department of ETH Zurich. First-order reversal curves (FORC) were measured on a PMC vibrating sample magnetometer (VSM) at 20 K, 50 K, and 90 K. The FORC data was

TABLE I. Peak temperatures (K) of the in-phase susceptibility χ' and the out-of-phase susceptibility χ'' for the mixed system HoSF-MNP and the individual components HoSF and MNP at different frequencies.

	Mixed system frequency (kHz)			Individual components frequency (kHz)		
	0.1	1	10	0.1	1	10
χ' (HoSF)	20	22	26	16	17	19
χ'' (HoSF)	11.5	12	14	11	12	14
χ' (MNP)	190	197.5	220	230	245	260
χ'' (MNP)	145	152.5	167.5	180	185	205

processed with a MATLAB code by Winklhofer and Pike (http://venu.geophysik.uni-muenchen.de/ michael/forcnew/).

III. EXPERIMENTAL RESULTS AND DISCUSSION

A. Induced magnetization as a function of temperature

Figures 1(a)–1(c) show the induced magnetization versus temperature measured in a 50 mT field for the two individual components and the mixed system. Figure 1(a) shows the measurements for pure HoSF, in which the maximum in the ZFC curve at 12 K indicates the average unblocking temperature of the ferritin.[8,13] The bifurcation point between ZFC and FC curves at 22 K shows the point in which all particles are unblocked. For the magnetite nanoparticles (MNP), the average unblocking temperature is at 56 K and the bifurcation point is at 125 K [Fig. 1(b)]. The shape of the curve resulting from the mixed system [Fig. 1(c)] is a combination of the curves in Figs. 1(a) and 1(b). The average unblocking temperature is at 15.6 K, indicating that the HoSF is the dominant component. The higher unblocking temperature observed for the mixed system compared to the pure HoSF, however, must be due to the magnetite particles. The gap between ZFC and FC curves at low temperature is a result of remanent magnetization acquired when cooling in a field. In the mixed system the distance between the ZFC and FC curves is relatively large in comparison to that of the individual components. The curves are separated below a temperature of 126 K, which corresponds to the final unblocking temperature of the magnetite nanoparticles. The decreasing separation of the curves during heating reveals the decreasing content of blocked particles in the system.[14]

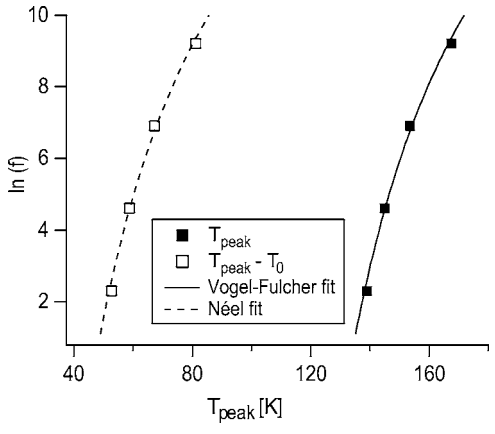

FIG. 4. Logarithm of measurement frequency $\ln(f)$ versus measured peak temperatures of χ'' for the HoSF-MNP mixed system (filled symbols) with a fit to the Vogel-Fulcher law (solid line). Néel relaxation for a noninteracting system would follow the peak temperatures corrected for T_0=86 K (open symbols).

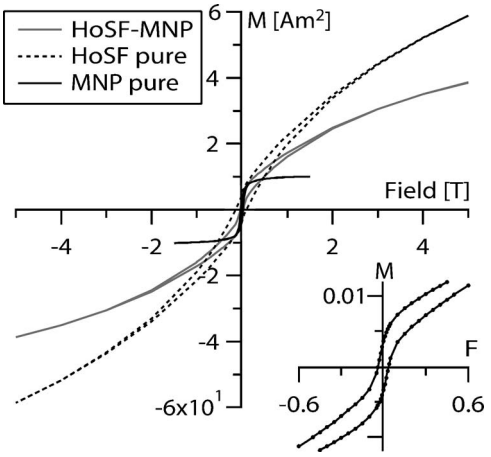

FIG. 5. Hysteresis measurements of the HoSF-MNP mixed system and the single components at 5 K. The inset shows the wasp-waisted shape of the hysteresis at low fields.

These results are compared to a natural sample of human brain tissue, which may contain a similar mixed system.[15] The dependence of magnetization induced in a 50 mT field on temperature is shown in Fig. 2. The effect of the strong diamagnetic matrix is obvious, since both the ZFC and the FC curve show a negative magnetization above 10 K (Fig. 2, inset). The diamagnetic signal, however, is independent of temperature and can be separated from other components. At temperatures below 5 K, the uncorrected curves show an increase with decreasing temperature due to a superposed paramagnetic contribution of the heme-iron of blood.[15] The measurements were corrected for a diamagnetic contribution of -1.64×10^{-4} A m^2/kg and a paramagnetic signal of 1.5 mg of freeze-dried blood. The local maximum in the corrected ZFC curve around 11 K is indicative of the average unblocking temperature of ferritin in the brain tissue. The slight gap between the ZFC and FC curves up to around 70 K indicates the influence of a remanent magnetization from an additional component, which is magnetite/maghemite.

B. ac susceptibility

Measurements of the in-phase (χ') and out-of-phase (χ'', quadrature) components of ac susceptibility for the HoSF-MNP system are shown in Figs. 3(a) and 3(b), respectively. Each of the components shows two distinct peaks in the susceptibility curve, which can be assigned to HoSF at lower temperature and to MNP at higher temperature. χ' displays a strong frequency dependence for both components. The peak temperatures increase with increasing frequencies while the signal strength decreases at higher frequencies. For χ'' the frequency dependence of the HoSF peak is less obvious,

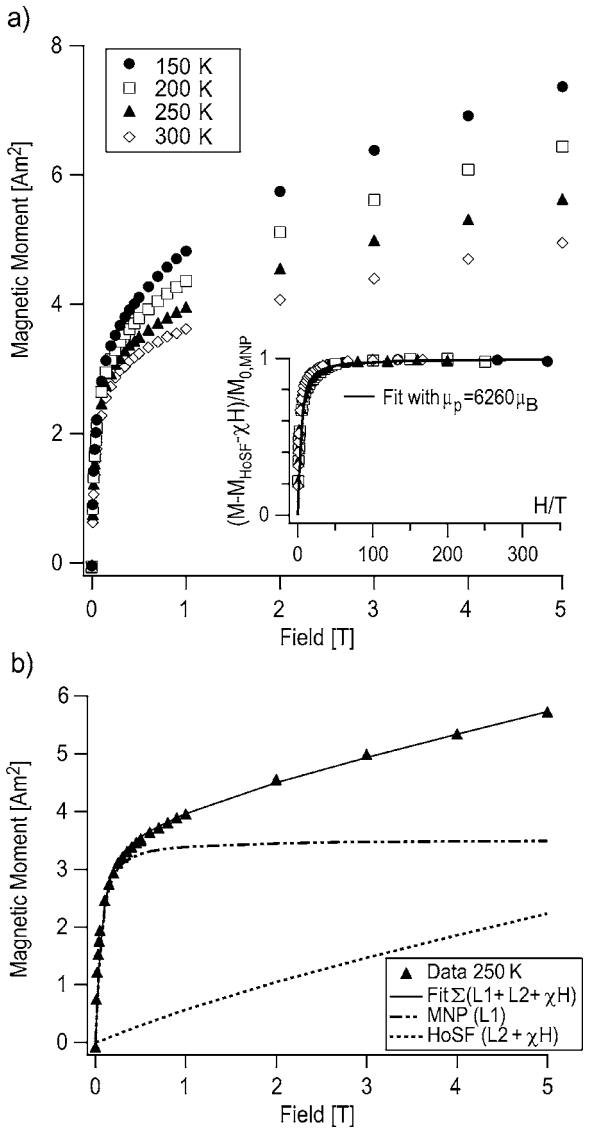

FIG. 6. (a) Initial magnetization curves as a function of field of the mixed system HoSF-MNP above temperatures required for full unblocking of both components. The inset shows $(M_{\mathrm{Mix}}-M_{\mathrm{HoSF}}-\chi H)/M_{0,\mathrm{MNP}}$ vs H/T. (b) Initial magnetization curve at 250 K and fit to Eq. (2) together with the initial magnetization of the separated components MNP and HoSF deduced from the fit.

while for the MNP peak the frequency dependence is strong [Fig. 3(b)]. All values of the peak temperatures are given in Table I. Comparing these to the values of the individual components [shown for 1 kHz in Figs. 3(a) and 3(b)], χ' of pure HoSF peaks at slightly lower temperature than the HoSF component in the mixed system. For χ'' the values for pure HoSF are almost identical with the χ'' in the mixed system. The opposite effect is observed for the MNP component. The pure MNP phase peak temperatures of χ' are significantly higher than for the MNP component, which corresponds to a shift towards lower temperatures in the mixed system. A similar shift is seen for χ''(Table I). A study of the average blocking temperature of ferrihydrite showed that by coating the nanoparticles with silicon, interaction is partially inhibited leading to a decrease in T_B.[16] A similar explanation may be valid for this system, where the magnetite concentration is less than 1% of the sample weight. The small amount of MNP, dispersed within the ferritin, reduces interactions between the MNP particles, thereby shifting the peak to lower temperatures.

TABLE II. Parameters for the individual components of HoSF and MNP from the fit to a sum of two Langevin functions [Eq. (2)] with $\mu_{\mathrm{p,MNP}}=6260\mu_B$ and $\mu_{\mathrm{p,HoSF}}=320\mu_B$ at temperatures above T_B.

	150 K	200 K	250 K	300 K
$M_{0,\mathrm{Mag}}$ (Am^2)	4.08	3.84	3.52	3.35
$M_{0,\mathrm{Ferr}}$ (Am^2)	0.88	0.51	0.49	0.23
$\chi\times10^{-9}$ (Am^2/T)	5.38	4.59	3.63	2.29

An indication that there is still interaction between the MNP particles within the mixed system is seen from the fact that the Arrhenius law $\tau=\tau_0\exp[E/kT]$ does not properly describe the relaxation peaks of χ''. For systems showing slight particle interactions, it has been proposed that the frequency-dependent peak susceptibility of χ'' would follow the Vogel-Fulcher equation,[17–20]

$$\tau=\tau_0\exp[E/k(T-T_0)]. \quad (1)$$

The measured peak temperatures of the MNP component are in good agreement with the Vogel-Fulcher law (Fig. 4) and the best-fit model yields $\tau_0=2\times10^{-9}$, $E/k=1016$ K, and $T_0=86$ K. These values for T_0 and E/k are very similar to values from other dispersed systems of biocompatible magnetite nanoparticle.[21] The fact that the measurements can be fitted by the Vogel-Fulcher law indicates that there are slight interactions between the magnetite nanoparticles. T_0 can be subtracted from the measured peak temperatures T_{peak} of χ'' to give the theoretical Néel relaxation peak temperatures in the absence of interactions (Fig. 4).

C. Induced magnetization versus field

At low temperature the hysteresis is dominated by the antiferromagnetic high coercivity HoSF component (Fig. 5). The MNP component leads to a clear wasp-waisted shape of the hysteresis loop (inset, Fig. 5) due to the mixing of a low coercivity component, such as magnetite, with a high coercivity component.[22] The hysteresis at 5 K of the HoSF-MNP system displays a coercive force (B_c) of 38 mT compared to values of 120 mT and 20 mT for pure HoSF and MNP, respectively. At higher temperature, B_c decreases from 38 mT (5 K) to 6 mT at 30 K, 3 mT at 50 K, and 0.5 mT at 100 K. At temperatures $\geq$150 K, the hysteresis is a closed loop and shows purely superparamagnetic behavior.

Initial magnetization curves at temperatures above full unblocking of the MNP are shown in Fig. 6(a). They are the result of two different superparamagnetic contributions, such that the initial magnetization curves must be fitted by a sum of a modified Langevin function and another Langevin function (one for HoSF and one for MNP),

$$M_{\mathrm{Mix}} = M_{0,\mathrm{MNP}} L_1(\mu_{\mathrm{p,MNP}} H/k_{\mathrm{B}}T) + M_{0,\mathrm{HoSF}} L_2(\mu_{\mathrm{p,HoSF}} H/k_{\mathrm{B}}T) + \chi H, \quad (2)$$

where $L=\coth x - 1/x$, $M_{0,\mathrm{MNP}}$ is the saturation magnetization of magnetite, $\mu_{\mathrm{p,MNP}}$ is the magnetic moment per magnetite nanoparticle, $M_{0,\mathrm{HoSF}}$ is the saturation magnetization of ferritin, $\mu_{\mathrm{p,HoSF}}$ is the magnetic moment per ferritin core, and χ is the high-field susceptibility. Using this model gives $\mu_{\mathrm{p,MNP}}=6260\mu_{\mathrm{B}}$ and a $\mu_{\mathrm{p,HoSF}}=320\mu_{\mathrm{B}}$. The small value for the horse spleen ferritin agrees with modeled values between $300\mu_{\mathrm{B}}$ and $350\mu_{\mathrm{B}}$ that are reported in the literature.[8,13,23] Fitting the initial magnetization curves to a sum of two Langevin functions [Eq. (2)] allows the total magnetic signal to be divided into the two separate components. An example is given for the data at 250 K in Fig. 6(b). Superparamagnetic MNP particles show saturation below 1 T, whereas "superantiferromagnetic" ferritin[24] is characterized by a continuous increase of magnetization with increasing field.[25] The linear part χH becomes weaker at higher temperature.[8,23] The signal of the MNP component can be deduced by subtracting the magnetization of the ferritin and plotting $(M_{\mathrm{Mix}}-M_{\mathrm{HoSF}}-\chi H)/M_{0,\mathrm{MNP}}$ versus H/T [inset, Fig. 6(a)]. It can be seen that the modified, initial magnetization curves collapse onto a single curve, indicating superparamagnetic behavior at temperatures above the peak ordering temperature.[26] It should be noted that $M_{0,\mathrm{Mag}}$, $M_{0,\mathrm{Ferr}}$, and χ are temperature dependent and decrease with increasing temperature (Table II).

D. First-order reversal curves (FORC)

FORC diagrams constitute a powerful method of displaying the grain-size dependence of hysteresis properties of natural and synthetic magnetic materials.[27] FORC measurements for the HoSF-MNP system are displayed in Figs. 7(a)–7(c). All diagrams show a pronounced density distribution of the microcoercivity around the origin that is due to the superparamagnetic contribution from particles that are unblocked.[28] At 20 K the ordered MNP component shows a maximum in the microcoercivity distribution (along B_{c} axis) at $B_{\mathrm{c}}=21$ mT, indicating the stable single-domain state of the MNP component [Fig. 7(a)]. The vertical spread in this distribution (along the B_{b} axis) is indicative of particle interaction. Although these particles are coated with a polypeptide and albumin, they still interact and cluster at low temperatures, as suggested by the susceptibility data. The HoSF component is largely responsible for the signal at $B_{\mathrm{c}}=0$, due to its superparamagnetic behavior. However some of the distribution along the B_{c} axis may also be attributed to HoSF, since it is only totally unblocked at 22 K. Continuous unblocking of both components is seen at higher temperature [Fig. 7(b)]. The maximum of microcoercivity from the MNP shifts towards the origin and the vertical spread decreases, reflecting a decrease in interaction as more magnetite particles are unblocked. The local maximum in coercivity distribution disappears completely at 90 K [Fig. 7(c)], where the FORC diagram is only dominated by the superparamagnetic contribution from both MNP and HoSF. The transition to superparamagnetism appears to occur at lower temperature than expected from the induced magnetization measurements [Fig. 1(c)]. This is probably due to the different measurement sensitivities of the two instruments. The signal for the FORC measurements was at the lower limit of the VSM, so that a relatively high smoothing factor was applied. This

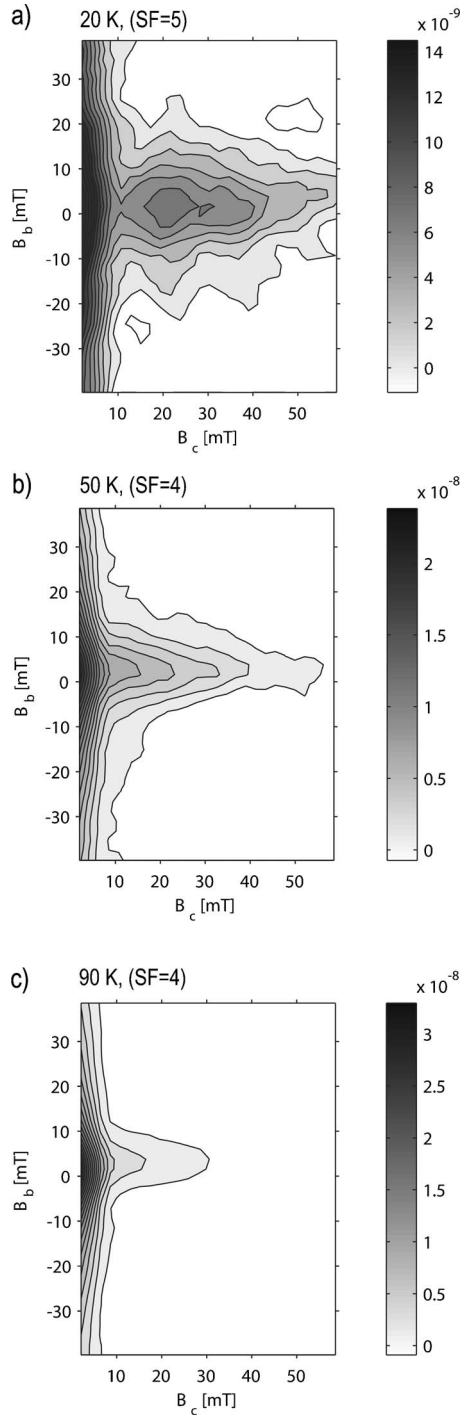

FIG. 7. FORC diagrams showing the effect of increasing temperature (a) at 20 K, single-domain peak due to MNP and broad superparamagnetic distribution near origin due to HoSF, (b) at 50 K, disappearing of single-domain component and increase of superparamagnetic signal due to conversion of MNP, and (c) at 90 K, purely superparamagnetic behavior of entire mixed system.

in turn acts effectively as a low pass filter of the data, which eliminates weaker features.[29]

IV. CONCLUDING REMARKS

The mixed system we have studied contains the high coercivity component ferritin and low coercivity component magnetite. In this mixture the ferritin dominates the magnetization at low temperatures in moderate to high fields, as demonstrated by induced magnetization and hysteresis analysis. The difference between ac susceptibility and the induced magnetization is that HoSF dominates the latter whereas MNP dominates the ac susceptibility. This observation demonstrates the power of using different measuring methods for a two-component system. The small remanent component in the antiferromagnetic HoSF is due to defect moments at the surface of the ferritin core. This is enhanced by the applied DC field of 50 mT. The weak ac field is more efficient, however, in activating the ferrimagnetic particles rather than activating the uncompensated spins.

Interaction between the MNP particles appears to be important, even though these particles are coated in albumin. This is seen from (i) the shift in peak temperatures in the mixed system as compared to the individual components in the dc susceptibility data; (ii) the fact that χ'' follows the Vogel-Fulcher law; and (iii) the spread along the B_b axis in the FORC diagram. The magnetic signals from a natural system may be much weaker than those of the synthetic mixture studied in this work; however, the results from the investigated mixed system, composed of a ferrimagnetic and an antiferromagnetic component, are similar to results from human brain tissues.[30] This observation indicates that such two-component magnetic models are useful for identifying the components of complex natural materials.

ACKNOWLEDGMENTS

We thank the Institute for Geosciences at the University of Bremen and the Department of Chemistry at ETH Zurich, especially Dr. Thomas Frederichs and Alois Weber for the use of the MPMS and PPMS, and very helpful discussions. We also thank Michael Winklhofer for the FORC analysis MATLAB code. Jon Dobson gratefully acknowledges the support of the Royal Society/Wolfson Foundation. The work of F. Brem and A. M. Hirt was supported under ETH Project No. 0-20118-03. Contribution nr. 1452, Institute of Geophysics, ETH Zurich.

*Corresponding author. Electronic address: hirt@mag.ig.erdw.ethz.ch

[1] A. M. Hirt, L. Lanci, J. Dobson, P. Weidler, and A. U. Gehring, J. Geophys. Res., [Solid Earth], **107**, 2011 (2002).
[2] U. Schwertmann, J. Friedl, H. Stanjek, and D. G. Schulze, Clay Miner. **35**, 613 (2000).
[3] J. Dobson, FEBS Lett. **496**, 1 (2001).
[4] A. Slawska-Waniewska, E. Mosiniewicz-Szablewska, N. Nedelko, J. Galazka-Friedman, and A. Friedman, J. Magn. Magn. Mater. **272**, 2417 (2004).
[5] N. D. Chasteen and P. M. Harrison, J. Struct. Biol. **126**, 182 (1999).
[6] J. L. Kirschvink, A. Kobayashi-Kirschvink, and B. J. Woodford, Proc. Natl. Acad. Sci. U.S.A. **89**, 7683 (1992).
[7] P. P. Schultheiss-Grassi and J. Dobson, BioMetals **12**, 67 (1999).
[8] S. A. Makhlouf, F. T. Parker, and A. E. Berkowitz, Phys. Rev. B **55**, R14717 (1997).
[9] P. D. Allen, T. G. St Pierre, W. Chua-anusorn, V. Strom, and K. V. Rao, Biochim. Biophys. Acta **1500**, 186 (2000).
[10] F. Brem, G. Stamm, and A. M. Hirt, J. Appl. Phys., **99**, to be published (2006).
[11] L. X. Tiefenauer, G. Kuhne, and R. Y. Andres, Bioconjugate Chem. **4**, 347 (1993).
[12] L. X. Tiefenauer, A. Tschirky, G. Kuhne, and R. Y. Andres, Magn. Reson. Imaging **14**, 391 (1996).
[13] M. S. Seehra and A. Punnoose, Phys. Rev. B **64**, 132410 (2001).
[14] H. Pardoe, W. Chua-anusorn, T. G. St Pierre, and J. Dobson, J. Magn. Magn. Mater. **225**, 41 (2001).
[15] F. Brem, A. M. Hirt, C. Simon, H. G. Wieser, and J. Dobson, BioMetals **18**, 191 (2005).
[16] J. Zhao, F. E. Huggins, Z. Feng, and G. P. Huffman, Phys. Rev. B **54**, 3403 (1996).
[17] S. Taketomi, Phys. Rev. E **57**, 3073 (1998).
[18] J. Zhang, C. Boyd, and W. Luo, Phys. Rev. Lett. **77**, 390 (1996).
[19] S. Shtrikman and E. P. Wohlfarth, Phys. Lett. **85**, 467 (1981).
[20] H. Shim, A. Manivannan, M. S. Seehra, K. M. Reddy, and A. Punnoose, J. Appl. Phys. **99**, 08Q503 (2006).
[21] P. C. Morais, J. G. Santos, L. B. Silveira, C. Gansau, N. Buske, W. C. Nunes, and J. P. Sinnecker, J. Magn. Magn. Mater. **272-276**, 2328 (2004).
[22] L. Tauxe, T. A. T. Mullender, and T. Pick, J. Geophys. Res., [Solid Earth], **101**, 571 (1996).
[23] S. H. Kilcoyne and R. Cywinski, J. Magn. Magn. Mater. **140**, 1466 (1995).
[24] C. Gilles, P. Bonville, H. Rakoto, J. M. Broto, K. K. W. Wong, and S. Mann, J. Magn. Magn. Mater. **241**, 430 (2002).
[25] M. S. Seehra, V. S. Babu, A. Manivannan, and J. W. Lynn, Phys. Rev. B **61**, 3513 (2000).
[26] P. Dutta, A. Manivannan, M. S. Seehra, N. Shah, and G. P. Huffman, Phys. Rev. B **70**, 174428 (2004).
[27] A. P. Roberts, C. R. Pike, and K. L. Verosub, J. Geophys. Res., [Solid Earth], **105**, 28461 (2000).
[28] C. R. Pike, A. P. Roberts, and K. L. Verosub, Geophys. J. Int. **145**, 721 (2001).
[29] D. Heslop and A. R. Muxworthy, J. Magn. Magn. Mater. **288**, 155 (2005).
[30] F. Brem, A. M. Hirt, C. Simon, H. G. Wieser, and J. Dobson, J. Phys.: Conf. Ser. **17**, 61 (2005).